



Simulation of An Asymmetric TM Metamaterial Waveguide Absorber

H. M. Mousa

Physics Department, Al Azhar University, Gaza strip. Palestinian Authority

e-mail:h.mousa@alazhar.edu.ps

ABSTRACT

This paper tackles the simulation of an asymmetric TM mode absorption in a lossy metamaterial (left-handed) slab (LHM) sandwiched between a lossy substrate and covered by a lossless dielectric cladding. The asymmetric solutions of the eigen value equation describe lossy $-$ guided modes with complex $-$ valued propagation constants. The dispersion relations, normalized field and the longitudinal attenuation were numerically solved for a given set of parameters: frequency range; film's thicknesses; and TM mode order. I found out that high order modes which are guided in thinner films are generally have more loss of power than low-order modes since the mode attenuation along z-axis α_z increases to negative values by the mode's order increase and the film thickness decrease. Moreover, LHM, at incident wavelength $=1.9 \mu m$, refractive index $=-3.74+i2$ and at thickness $=0.3 \mu m$, guides the power better than RHM or metal one. This LHM is appropriate for solar cell applications. For arbitrary LHM, at frequency band of wavelength (600, 700 to 1200) nm, the best absorption is attained at longer wavelengths and for lower order modes at wider films.

KEYWORDS: Attenuation; Eigen-value equation; Left handed material; Solar cells.



Council for Innovative Research

Peer Review Research Publishing System

Journal: Journal of Advances in Physics

Vol 4, No.3

japeditor@gmail.com

www.cirjap.com

1. INTRODUCTION

Recently, the so-called left handed material (LHM), or meta-material whose unit cell is devised to show unnatural electromagnetic (EM) properties applicable to advanced devices, have attracted great interest for research [1–6]. The manipulation of effective parameters for the artificial medium diversifies the application of LHM. One of them, the perfect absorption (PA), which is potentially used for sensing [7] and solar energy [8], has become one of the significant issues related to LHM. The initial PA was demonstrated for the GHz regime by Landy et al [9] in 2008. To date, PAs have been developed in every relevant spectral range, from microwave [9], THz [7], near-IR [10], to the near-optical. The problem of wave guidance in amplifying media has been analyzed [11] and has proved very useful in the field of semiconductor lasers. This problem is mathematically analogous to that of wave guidance in lossy substrate which is encountered in the field of thin film photovoltaics. The goal of photovoltaic structures is to absorb as much light as possible within specific layers. James et.al. [12,13] examined the problem of lossy waveguide propagation and derives the full-field solution to the problem of wave guidance in a symmetric and an asymmetric three layer slab. They explored lossy mode propagation in the context of photovoltaics by modeling a thin film solar cell made of a morphous silicon (right handed material (RHM)). During the past decade, there has been a phenomenal growth in the understanding and applications of meta-materials [14]. Meta-materials are composite structured materials, structured at sub-wavelength scales, and depend on the structure to give rise to electromagnetic resonances. Due to the resonant behavior, meta-materials can exhibit extreme values of the effective medium parameters such as large and/or negative dielectric permittivity [15] and permeability [16]. The design of absorptive meta-materials can be scaled from microwave [17] and terahertz [18] through the infrared [19] almost into optical frequencies [20]. Optimized meta-materials with high absorption have been proposed for applications such as thermal spatial light modulators [19], plasmonic sensors [21], thermal bolometers [22] and solar thermo-photo-voltaics [23]. S. Zhang et.al. [24] numerically demonstrated a meta-material with both negative permittivity and negative permeability over an overlapping near-infrared wavelength range resulting in a low loss negative-index material and thus a much higher transmission, which will lead to more extensive applications. The negative index material consists of a pair of gold films separated by a dielectric layer with a two dimensional square periodic array of circular holes performing the entire multilayer structure. The negative refractive index was obtained at a wavelength around 2000nm , the real part is as negative as -2 . Furthermore, the proposed structure has a minimum feature size of $\sim 100\text{nm}$. This paper examines the problem of lossy waveguide absorption when (LHM) is implemented as lossy thin film in an asymmetric waveguide. The basic structure of interest for this work is the planer three-layered dielectric structure depicted in Fig. (1). It consists of LHM slab with thickness $2h$ covered by a lossless dielectric cladding of real refractive index n_c . The substrate is lossy with complex index of $\tilde{n}_s = n_s + ik_s$. LHM film is lossy and has a complex index of refraction $\tilde{n}_h = -\sqrt{\mu_h \epsilon_h} + ik_h$. The simulations are also performed for another arbitrary LHM which has negative index in the visible region of frequency band at wavelength of value (600, 700 to 1200 nm).

2. DERIVATION OF THE EIGEN –VALUE EQUATION:

The propagation of TM waves through a thin lossy film of (LHM) with thickness $2h$ covered by a lossless cladding is considered. LHM film occupies the region $-h < x < h$. The cladding occupies the region $x > h$, and the substrate in the region $x < -h$.

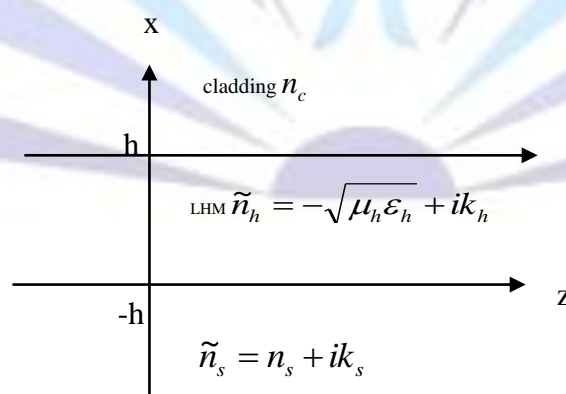


Fig.1: Waveguide Configuration for a lossy asymmetry LHM waveguide.

I present the eigen value equation for transverse electric (TE) waves propagating in the z direction with a propagation wave constant in the form $\exp[i(k_z z - 2\pi ft)]$, f is the operating frequency. The electric and magnetic field vectors for TE waves propagating along z -axis with angular frequency ω and wave number k_z are defined as [5,6]:



$$\begin{aligned} H &= [0, H_y(\omega, z), 0] \exp i(k_z z - \omega t) \\ E &= [E_x(\omega, z), 0, E_z(\omega, z)] \exp i(k_z z - \omega t) \end{aligned} \quad (1)$$

2.1 In lossy LH film, $-h < x < h$

The wave equation can be found easily from the Maxwell's equations as :

$$\frac{\partial^2 H_y}{\partial x^2} - k_z^2 H_y + k_h^2 H_y = 0 \quad (2)$$

Where $k_h = k_0 \tilde{n}_h$ and , $\tilde{n}_h = -\sqrt{\mu_h \varepsilon_h} + ik$ is refractive index of LH film. ε_h , μ_h is the electric permittivity and magnetic permeability of LHM respectively .

$k_z = \beta_z + i\alpha_z$, where β_z is the longitudinal phase constant , α_z is the mode attenuation coefficient along z-axis, $k_0 = 2\pi / \lambda$ is the wave propagation length in free space and λ is the free-space wavelength for the model.

The asymmetric solution of Eq(2) has the form[12]:

$$H_y = H_0 e^{ik_z z} [e^{ik_x x} + B e^{-ik_x x}] \quad (3)$$

$$E_z = (-1 / \omega \varepsilon_0 \tilde{n}_h^2) H_0 k_x e^{ik_z z} [e^{ik_x x} - B e^{-ik_x x}] \quad (4)$$

If this solution is substituted into Eq.(2) the resulted relation is

$$k_h^2 = k_x^2 + k_z^2 \quad (5)$$

2.2. In lossless cladding, $x > h$

The wave equation is:

$$\frac{\partial^2 H_y}{\partial x^2} + (k_c^2 - k_z^2) H_y = 0 \quad (6)$$

Where, $k_c = k_0 n_c$ is the wave number of the cladding region.

The asymmetric solution for Eq.(6) is given by [12]

$$H_y = A H_0 e^{ik_z z} e^{i\gamma_c(x-h)} \quad (7)$$

$$E_z = (-\gamma_c / \omega \varepsilon_0 n_c^2) H_0 A e^{ik_z z} e^{i\gamma_c(x-h)} \quad (8)$$

A is a constant determined by boundary conditions and

γ_c is the complex propagation constant, the real component of it causes the phase oscillation with respect to x-axis. It satisfies the relation

$$k_c^2 = k_z^2 + \gamma_c^2 \quad (9)$$

$n_c = \sqrt{\varepsilon_c \mu_c}$ with magnetic permeability $\mu_c = 1$, ε_c is the electric permittivity of the cladding .

2.3. In lossy substrate, $x < -h$

The wave equation is:



$$\frac{\partial^2 H_y}{\partial x^2} + (k_s^2 - k_z^2)H_y = 0 \tag{10}$$

Where, $k_s = k_0 \tilde{n}_s$ is the wave number of the substrate region.

The asymmetric solution for Eq.(10) is given by [25]

$$H_y = CH_0 e^{ik_z z} e^{-i\gamma_s(x+h)} \tag{11}$$

$$E_z = (\gamma_s / \omega \epsilon_0 \tilde{n}_s^2) H_0 C e^{ik_z z} e^{-i\gamma_s(x+h)} \tag{12}$$

γ_s is the complex propagation constant. It satisfies the relation

$$k_s^2 = k_z^2 + \gamma_s^2 \tag{13}$$

$n_s = \sqrt{\epsilon_s \mu_s}$ with magnetic permeability $\mu_s = 1$, ϵ_s is the electric permittivity of the substrate .

The continuity of H_y and E_z at the boundary $x = -h$ leads to the following equations

$$e^{-ik_x h} + B e^{ik_x h} = C \tag{14}$$

$$e^{-ik_x h} - B e^{ik_x h} = -\gamma_s C \tilde{n}_h^2 / k_x \tilde{n}_s^2 \tag{15}$$

The continuity of H_y and E_z at the boundary $x = h$ leads to the following equations

$$e^{ik_x h} + B e^{-ik_x h} = A \tag{16}$$

$$e^{ik_x h} - B e^{-ik_x h} = \gamma_c A \tilde{n}_h^2 / \tilde{n}_c^2 k_x \tag{17}$$

Using a little manipulation and substitution, the TM asymmetric eigen value equation is obtained as:

$$e^{i4k_x h} = \frac{(k_x \tilde{n}_s^2 + \gamma_s \tilde{n}_h^2)(k_x n_c^2 + \gamma_c \tilde{n}_h^2)}{(\tilde{n}_s^2 n_c^2 k_x^2 - k_x \gamma_c \tilde{n}_h^2 \tilde{n}_s^2 - n_c^2 \tilde{n}_h^2 \gamma_s k_x + \tilde{n}_h^4 \gamma_s \gamma_c)} \tag{18}$$

And

$$B = \frac{(n_c^2 k_x - \gamma_c n_h^2) e^{2ik_x h}}{(n_c^2 k_x + \gamma_c n_h^2)} \tag{19}$$

By Eq.(5), Eq.(9)and Eq.(13),

$$\begin{aligned} \gamma_c &= \sqrt{k_c^2 - k_h^2 + k_x^2} \\ \gamma_s &= \sqrt{k_s^2 - k_h^2 + k_x^2} \end{aligned} \tag{20}$$

Equation(18) determines the allowed values for the TM complex wave number of asymmetric modes . Since the eigen value equation is transcendental , it can only solved through iterative methods. I used Steepest descent method with linear line search[12]. Values of k_x which satisfy the eigen value equation(18)can then be back-substituted to solve for all other propagation constants and generate the total TM field solutions over all space.



3. NUMERICAL RESULTS AND DISCUSSION:

Near infrared frequencies, such as 160 THz ($\lambda = 1.9 \mu m$) LHM has $\epsilon_h = -14, \mu_h = -1$ [24] and refractive index, $\tilde{n}_h = -\sqrt{\epsilon_h \mu_h} + i2 = -3.74 + i2$, the cladding refractive index $n_c = 1$ and substrate refractive index $\tilde{n}_s = 1.26 + i7.2$, the dispersion equation (18) has been solved to compute the complex wave numbers of the modes. At the film thickness $h = 0.5 \mu m$, Fig.(2a) displays the corresponding electric field profile (normalized to unit amplitude) for the modes of lossy (LHM) waveguide i.e. (M=3, M=4 and M= 5). The resultant propagation constants are summarized in Table 1.

Table 1. Propagation constants of TM mode(3, 4, 5) solutions to LHM waveguide of $h = 0.5 \mu m$. The parameters are of unit μm^{-1}

Mode	k_x	k_z	γ_c	γ_s
3	5.794-i0.6	11.46-i7.44	7.419+i11	6.964+i25.99
4	6.943-i0.324	10.95-i7.6	7.79+i10.49	7+i25.68
5	8.647+i0.658	10.32-i8.47	8.4+i9.7	7.179+i25.2

It is shown that in both LHM film ($-0.5 < x < 0.5$) and the substrate region ($-1 < x < -0.5$), the normalized magnetic field increases by the mode's order increase to the value of (3, 4, 5). This is because of the real part increase of both the propagation number k_x and γ_s to the values of (5.794, 6.943, 8.647) and (6.964, 7, 7.179) for M =3, 4, 5 respectively. In LHM film, the normalized magnetic field is trapped and increases to the values of (0.55, 0.65, 1.4)A/m for the previous modes. The increasing values of the longitudinal attenuation α_z (imaginary part of k_z) is important to the field of light trapping in thin films, as it represents the absorption length of a guided mode in the structure. Negative α_z means loss of wave power from the structure while positive α_z means absorption of wave power by the structure. By increasing α_z to the values of (-7.44, -7.6, -8.47) for M =3, 4, 5 respectively, the modes have negative absorption lengths and the most loss of the power from the structure is observed for M=5. The normalized magnetic field in the film is of value 1.4 for M=5 which means absorption of the wave is achieved in LHM film as well as a dramatic evanescent decay in the cladding region ($0.5 < x < 1$) and wasting its power in the substrate. In Fig.(2b) the magnetic field profile is plotted (normalized to unit amplitude) for the previous modes of lossy (LHM) waveguide for the film thickness $h = 0.3 \mu m$. It is observed that as h decreases, α_z increases to the values of (-8.88, -10.42, -11.96) with mode's order as shown by table 2 which means more loss of the magnetic energy from the structure is achieved.

Table 2. Propagation constants of TM mode(3,4,5) solutions to LHM waveguide of $h = 0.3 \mu m$. The parameters are of unit μm^{-1}

Mode	k_x	k_z	γ_c	γ_s
3	9.11-i1.07	10.3-i8.88	8.64+i9.46	7.22+i25.05
4	12+i0.54	8.48-i10.42	10.35+i7.89	7.56+i23.93
5	13.8+i0.95	7.9-i11.96	12.1+i6.7	7.9+i22.8

Fig. (3) describes the variation of mode attenuation along z-axis α_z with mode's order for different LHM thickness. It is noticed that, at $h = 0.3 \mu m$, high order modes are generally have more loss than low-order modes since the mode attenuation along z-axis α_z increases to the values of (-6.6 to -12) with the mode's number of (0 to 6). Besides that, the



attenuation increases to negative values by thickness decrease to the values $(0.7, 0.5, 0.3)\mu m$ i.e., for $M=6$, as h decreases to the values of $(0.7, 0.5, 0.3)\mu m$, α_z increases to the values of $(-7.3, -8.2, -12)$ respectively. Fig.(4a,b), displays a comparison of normalized magnetic field profile of $M=1$ mode of LHM with that of RHM(amorphous silicon) and with that of a metal, at $\lambda = 1.9\mu m$, and $h = 0.3\mu m$. The refractive index of the LHM is $n_h = -3.74 + i2$ [16] and that's of amorphous silicon film[RHM][12,13] is $n_f = 4.9 + i0.3$ and that's of metal film is assumed to be $n_m = -100 + i0.3$. The computed wave numbers for mode $M=1$ are summarized in Table 3

Table 3. Propagation constants of TM mode(M=1) solutions to LHM, RHM and metal waveguide at $h = 0.3\mu m$. The parameters are of unit μm^{-1} .

Film	k_x	k_z	γ_c	γ_s
LHM	4.625+i0.88	11.87-i7.23	7.146+i11.44	6.9+i26.23
RHM	6.09-i0.22	15.029+i1.16	1.08-i14.83	2.96+i28
Metal	$10.47+0.66 \times 10^{-3}$	330.5-i0.99	0.99+i330	1.29+i331.3

It is shown that, the normalized magnetic field of LHM is amplified in the film to the value of (1.6 A/m) and decays sharply in substrate and cladding. In RHM film, the amplifying of the field occurred of value (2.2 A/m) while in the cladding it reaches more greater than (-4 V/m) which leads to wasting of the power in the cladding. This is because α_z of RHM is (+1.16) while for LHM it is (-7.23) and of metal (-0.99) as shown by table (3). However, the magnetic field distribution shown in Fig. 4(a,b) clearly indicates the localization of magnetic field in the LHM layer which guides the power better than RHM or metal one. LHM structure guides the power through the film more than wasting it in the cladding as in RHM structure.

The complex dielectric constant of arbitrary LHM at optical frequencies is approximated by the Drude model as follows[26]

$$\epsilon = \epsilon_{lattice} - \frac{\omega_p^2}{\omega^2 + i\omega\gamma} \tag{21}$$

Where ω is the angular frequency, $\epsilon_{lattice}$ is the lattice permittivity, ω_p is the effective plasma frequency and γ is the electric damping factor, $\omega_p = 1.2 \times 10^{16} \text{ rad/s}$, $\gamma = 1.2 \times 10^{14} \text{ rad/s}$, $\epsilon_{lattice} = 9.1$. The calculations are performed for electromagnetic radiations in the visible regions at wavelength 600, 700 to 900 nm. In this frequency band the real part of refractive indices of arbitrary LHM according to(21) are -2.338, -3.274 to -4.86 while the permeability of LHM is assumed to be -1. Fig. 5 displays the magnetic field profile of the mode's order 4 at $h = 0.3\mu m$ for different wavelengths. It is observed that by the wavelength decrease to the values of (1200, 900, 600) nm, the magnetic field of the mode trapped in the film increases to the values of (0.24, 0.4, 0.68) respectively accompanied by more wasting in the substrate as a result of α_z increase to the values of (-10.93, -14.7, -22.549) which means the best absorption is attained at longer wavelength. As shown by Fig(6) longitudinal attenuations are computed and illustrated as a function of wavelength of the incident waves in the visible regions for TM mode's number $M=(1, 3, 5, 7)$ of arbitrary LHM model at $h = 0.3\mu m$. It is observed that the attenuation in this frequency band increases to negative values with the wavelength decrease and mode's order increase. At wavelength(600nm), α_z increases to the values of (-21.2, -22, -23.4, -25.4) μm^{-1} by mode's order M increase to(1, 3, 5, 7). This implies the best absorption is achieved for lower order modes. In Figure 7, we explore the effect of the film thickness on the mode attenuation α_z for arbitrary LHM model for $M=1$. It displays that attenuation increases to negative values with thickness decrease, which means the thinner the film, the mode will suffer more loss upon propagation in this structure.

4.CONCLUSIONS:

I investigated and simulated the modal dispersion relation and attenuation of TM modes in an asymmetric slab waveguide constructed from lossy thin LH film sandwiched between a lossy substrate and covered by a losseless dielectric cladding. The numerical solutions showed that, high order modes which are guided in thinner films are generally have more loss of power than low-order modes since the mode attenuation along z-axis α_z increases to negative values by the mode's order



increase and the film thickness decrease . LHM , at incident wavelength $=1.9 \mu\text{m}$ and at thickness $h=0.3\mu\text{m}$, is appropriate for solar cell applications since it guides the power better than RHM or metal one . For arbitrary LHM, the best absorption is attained at longer wavelengths in the considered frequency band and for lower order modes at wider films. This study will make a foundation for the creation of new optical technologies using "nanostructured metamaterials" with potential applications including advanced solar cells.

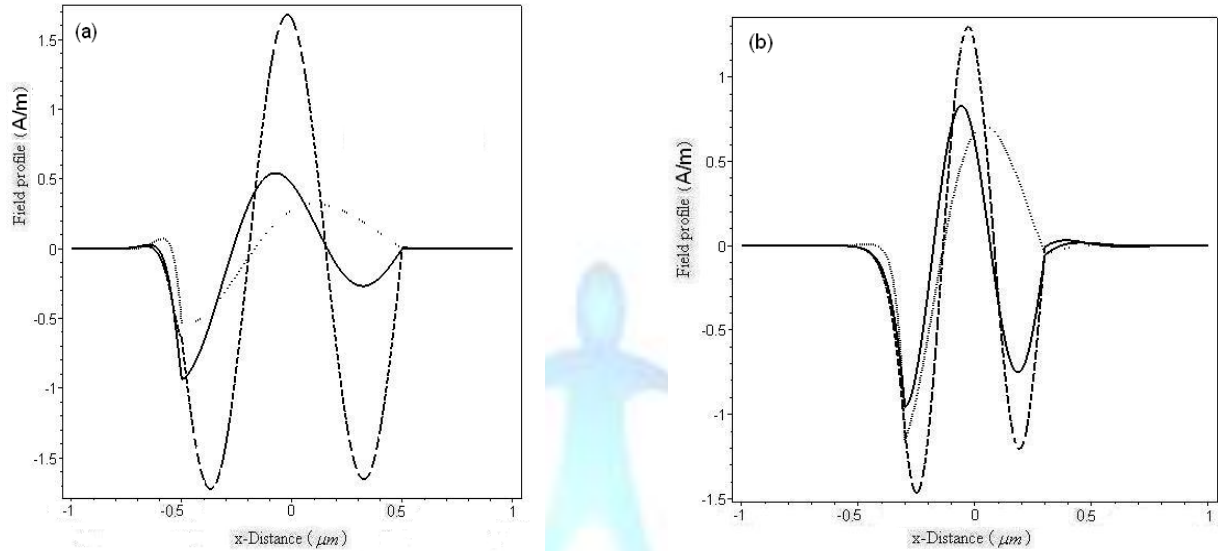


Fig.2(a,b): Magnetic field profile (normalized to unit amplitude) of the M=3(dotted), M=4(solid) and M=5 (dashed) mode for LHM model, at (a) $h = 0.5 \mu\text{m}$ and (b) $h = 0.3 \mu\text{m}$, $\tilde{n}_h = -3.74 + i2$, $\tilde{n}_s = 1.26 + i7.2$, $n_c = 1$, $\lambda = 1.9 \mu\text{m}$

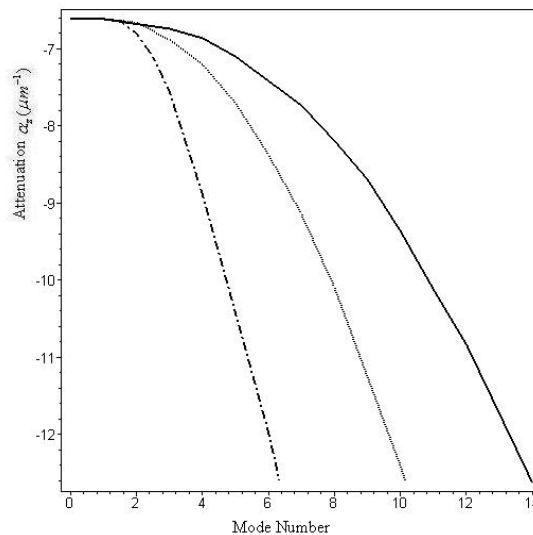


Fig.3 : Longitudinal attenuation coefficient (α_z) versus mode's number for different LHM thicknesses. $h = 0.7 \mu\text{m}$ (solid), $h = 0.5 \mu\text{m}$ (dotted), $h = 0.3 \mu\text{m}$ (dot dash)LHM model, $\tilde{n}_h = -3.74 + i2$, $\tilde{n}_s = 1.26 + i7.2$, $n_c = 1$, $\lambda = 1.9 \mu\text{m}$.

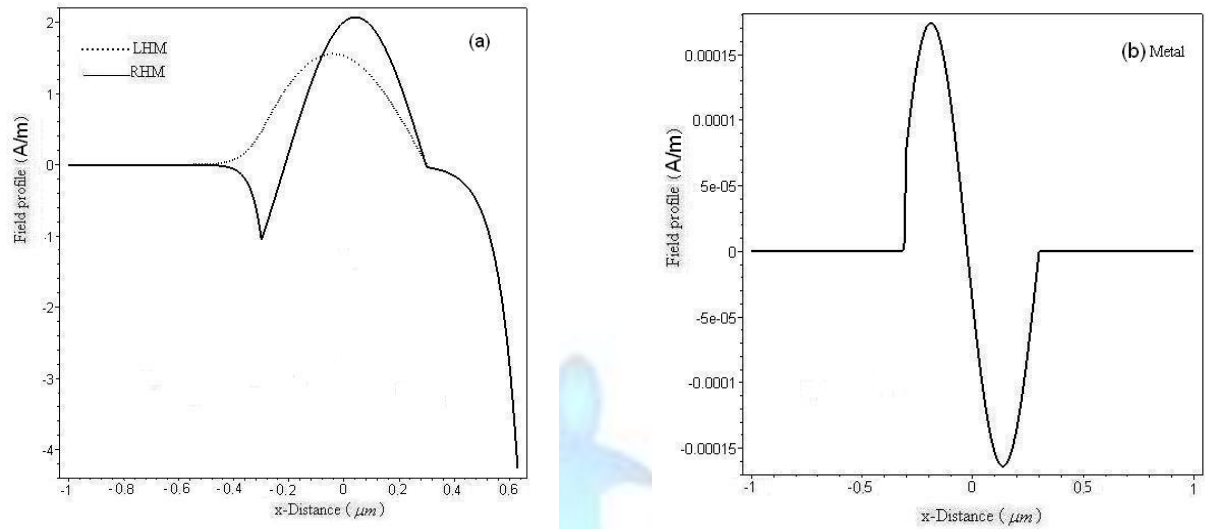


Fig.4(a,b): (a) Magnetic field profile of the M=1 mode at $h = 0.3\mu\text{m}$, $\lambda = 1.9\mu\text{m}$, $\tilde{n}_s = 1.26 + i7.2$, $n_c = 1$, where $\tilde{n}_h = -3.74 + i2$ for LHM model, $n_f = 4.9 + i0.3$ for RHM, and (b) for metal $n_m = -100 + i0.3$

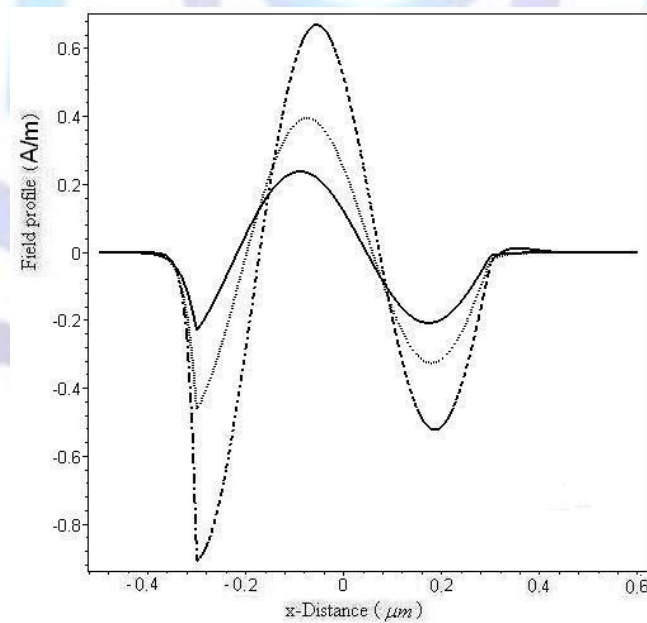


Fig.5 : Magnetic field profile of the M=4 mode at $h = 0.3\mu\text{m}$ for wavelength $\lambda = 600\text{nm}$ (dashdot), $\lambda = 900\text{nm}$ (dotted), and $\lambda = 1200\text{nm}$ (solid) of arbitrary LHM model for , $h = 0.3\mu\text{m}$, $n_c = 1$, $\tilde{n}_s = 1.26 + i7.2$

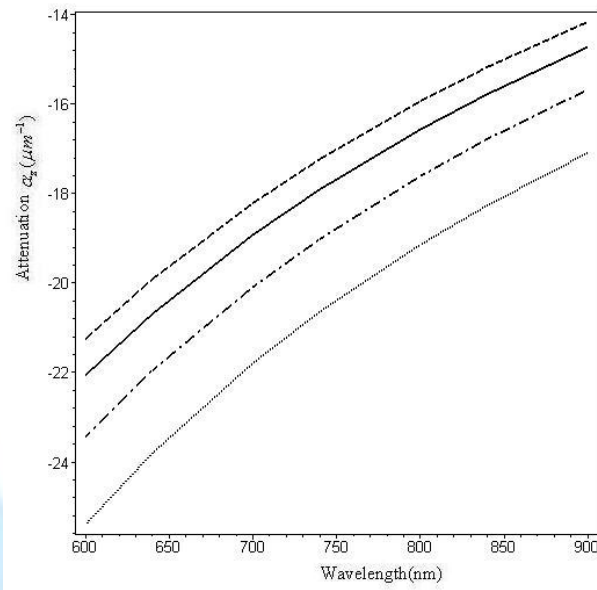


Fig.6: Longitudinal attenuation coefficient (α_z) of TM waves versus wavelength for mode's number $M=1$ (dashed), $M=3$ (solid), $M=5$ (dashdot), $M=7$ (dotted) of arbitrary LHM model for , $h = 0.3 \mu\text{m}$, $n_c = 1$, $\tilde{n}_s = 1.26 + i7.2$

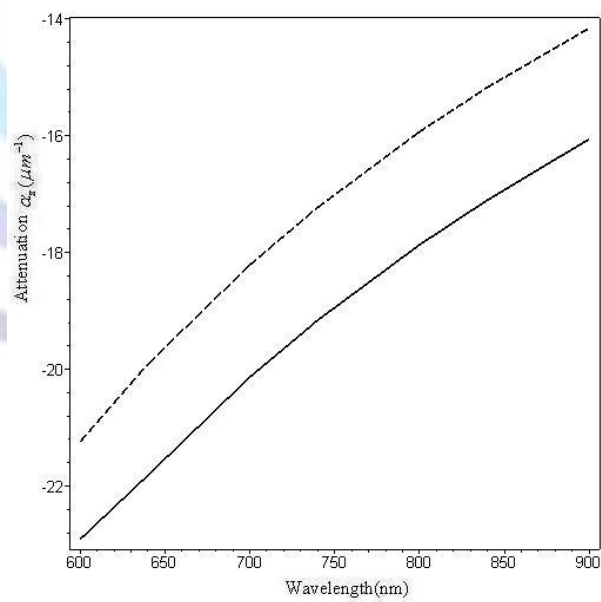


Fig.7: Longitudinal attenuation coefficient (α_z) of TM waves versus wavelength of mode's number $M=1$ for $h = 0.3 \mu\text{m}$ (dashed), $h = 0.1 \mu\text{m}$ (solid) of arbitrary LHM model $n_c = 1$, $\tilde{n}_s = 1.26 + i7.2$



REFERENCES

- [1] Krishnamoorthy, H. N. S, Jacob, Z., Narimanov, E. , Kretzschmar, I. and Menon V. M. 2012. Active plasmonics and tuneable plasmonic meta- materials. *Science* 336 .
- [2] Watts, C. M ., Liu, X . and Padilla, W .J.. Metamaterial Electromagnetic Wave Absorbers. 2012 *Adv .Mate .* 24,23, OP181.
- [3] Lu, Y. , Jin,X ., Lee,S. , Rhee J. Y. , Jang, W. H. and Lee, Y. P. , 2010.Passive and active control of a plasmonic mimic of electromagnetically induced transparency in stereo metamaterials and planar metamaterials. *Adv.Nat. Sci. Nanosci Nanotechnol.* 1 045004.
- [4] Pham, V. T. Park ,J. W. , Vu, D. L. , Zheng, H. Y., Rhee, J. Y. , Kim, K. W. and Lee,,Y. P. , 2013.THz- meta – material absorbers. *Adv. Nat. Sci.: Nanosci .Nanotechnol.* 4,1, 015001 .
- [5] Mousa, H. M. and Shabat, M. M.2012. TMwaves in cylindrical superlattices(LANS) bounded by left- handed material (LHM).*Appl. Phys.A,* 111, 1057-1063.
- [6] Mousa, H. M. and Shabat, M. M,2011. Electromagnetic guided waves in a metamaterial-magnetic waveguide structure. *Int. J. Modern Physics B,* 25 (32) .
- [7] Liu, N. , Mesch, M. , Weiss, T. , Hentschel,M. , and Giessen, H. , 2010, Infrared perfect absorber and its application as plasmonic sensor . *Nano.Lett.* 10, 2342.
- [8] Aydin, K. , Ferry,V. E. , Briggs, R. M. and Atwater, H. A. 2011.Broadband, polarization- independent resonant light absorption using ultrathin, plasmonic super absorbers. *Nature Commun.* 2, 517.
- [9] Landy, N. I. , Sajuyigbe, S. S, Mock, J. J. , Smith,D. R. , and Padilla,W. J. 2008. Perfect metamaterial absorber. *Phys. Rev.Lett.* 100 , 207402.
- [10] Dayal*,G. and Ramakrishna, S. A. 2012. Design of highly absorbing metamaterials for Infrared frequencies. *Opt.Express,*20,16 , 17503.
- [11] Siegman, A. E. 2003.Propagation modes in gain guided optical fibers. *J. Opt. Soc. Am. A ,* 20,1617-1628.
- [12] Nagel, J. R. , Blair,S. , and Scarpulla, M. A. 2011.Exact field solution to guided wave propagation in lossy thin films. *Optics Express ,*19,(21) , 20159.
- [13] Nagel, J. R. , Blair,S. , and Scarpulla, M. A, 2012.Exact field solution to guided wave propagation in lossy thin films. *Proc. Of SPIE ,*8256, 825606-1.
- [14] Ramakrishna, S. A. and Grzegorzcyk, T. M. ,2008. Physics and Applications of Negative Refractive Index Materials.(CRC Press, Boca Raton .
- [15] Pendry, J. B. , Holden, A. J. , Stewart,W. J. , and Youngs, I. 1996. Extremely Low Frequency Plasmons in Metallic Mesostructures. *Phys. Rev. Lett.* 76, 4773-4776.
- [16] Pendry, J. B. , Holden, A. J, Robbins, D. J. , and Stewart, W. J. 1999.Low frequency plasmons in thin-wire structures. *J. Phys. Condens. Matter* 10, 4785-4809.
- [17] Landy N. I., Sajuyigbe, S. , Mock, J. J. , Smith, D. R. , and Padilla, W. J. 2008. Perfect metamaterial absorber.*Phys. Rev.Lett.* 100, 207402 .
- [18] Tao, H. , Landy, N. I. , Bingham, C. M. Zhang, X. , Averitt, R. D. , and Padilla W. J. 2008.A metamaterial absorber for the terahertz regime: design. fabrication and characterization, *Opt. Express* 16, 7181-7188.
- [19] Liu, X. , Starr, T. , Starr ,A. F. Starr and Padilla, W. J. , 2010. Infrared spatial and frequency selective metamaterial with nearunity absorbance.*Phys. Rev. Lett.* 104, 207403.
- [20] Hao, J. , Wang, J. , Liu, X. , . Padilla, W. J. , Zhou, L. and Qiu,M. , 2010. High performance optical absorber based on a plasmonic metamaterial. *Appl. Phys. Lett.* 96, 251104 .
- [21] Liu,N. Mesch, M. , Weiss, T. , Hentschel, M. , and Giessen, H. 2010.Infrared perfect absorber and its application as plasmonic sensor. *Nano Lett.* 10, , 2342-2348.
- [22] Maier, T. and Brueckl, H. , 2010.Multispectral microbolometers for the mid infra-red.*Opt. Lett.* 35, 3766-3768.
- [23] Wu, C. , Neuner, B. , John, J. , Milder, A. , Zollars B. , Savoy, S. and Shvets, G. ,2012. Metamaterial-based integrated plasmonic absorber/emitter for solar thermo-photovoltaic systems.*J. Opt.*14, 024005 .
- [24] Zhang, S. , Fan, W., Malloy, K. J. and Brueck, S. R. J. , 2005. Near-infrared double negative metamaterials. *Optics Express,* 13,(13), 4922-4930. .
- [25] Balanis, C. A. 1989. *Advanced Engineering Electromagnetics*(Wiley, New York, NY,.
- [26] Isaac, TH. 2009, Thesis (PhD),University of Exeter,UK, "Tunable plasmonic structures for terahertz frequencies,